Thermal Effects on Deformability and Strengths of Maha Sarakham Salt

Sarayuth Aracheeploha, Decho Phueakphum and Kittitep Fuenkajorn

Geomechanics Research Unit, Institute of Engineering, Suranaree University of Technology,

Muang District, Nakhon Ratchasima, Thailand 30000.

Phone (66-44) 223-363, Fax (66-44) 224-448

E-Mail: kittitep@sut.ac.th

Abstract

A multi-axial strength criterion is developed to describe the distortional strain energy density of rock salt at failure as a function of the mean strain energy. The temperature effect on salt strength is implicitly considered by incorporating empirical relations between the elastic parameters and temperatures of the tested specimens. The proposed criterion agrees well with the test results obtained under temperatures ranging from 273 to 467 Kelvin. The proposed criterion is useful and practical for a conservative determination of the stability of compressed-air or gas storage caverns where the surrounding salt is subject to fluctuation of temperatures during product injection and withdrawal periods.

1. Introductions

The effects of temperature on deformability and strength of rocks have long been recognized [1-3]. It has been found that rock strength and elastic properties decrease as the temperature increases. For rock salt studies on the temperature effect have been concentrated on the time-dependent deformation (creep) [4, 5] where the results are specifically applied to assess the long-term performance of the nuclear waste repository in salt mass. Several complex formulations have been proposed to describe the thermo-mechanical behavior of rock salt under the repository environment. Such formulations are complex and require several material parameters that are difficult to obtain, and hence their applications are not truly practical for the mining industry. In addition the experimental and theoretical studies on the effect of temperature on the strengths of rock salt have been rare. Such knowledge is necessary for the design and stability analysis of salt around compressed-air and natural gas storage caverns [6].

The objective of this study is to develop a multi-axial strength criterion for rock salt under various temperatures and confining pressures. The predictability of the proposed criterion is verified by the results of uniaxial and triaxial compressive strength and Brazilian tensile strength tests on rock salt specimens subject to nominal temperatures ranging from 273, 298, 404 to 467 Kelvin (0-194 Celsius).

2. Salt Specimens

The salt specimens were prepared from 100 mm salt cores drilled from the depth ranging between 70 m and 100 m by Asean Potash Mining Co. in the Khorat basin, northeast Thailand. The salt cores belong to the Middle salt member of the Maha Sarakham formation [7]. The salt formation hosts several solution-mined caverns, and is considered as a host rock for compressed-air energy storage caverns by the Thai Department of Energy, and for chemical waste disposal by the Office of Atomic Energy for Peace [8, 9]. The salt cores used here are virtually pure halite with average grain (crystal) sizes of 5×5×10 mm^3. For the compression testing the cores were dry-cut to obtain cubical shaped specimens with nominal dimensions of 5.4×5.4×5.4 cm^3. The Brazilian test specimens were machined using a lathe to obtain 48 mm diameter circular disks with a thickness of 24 mm. No bedding is observed in the specimens.

RECEIVED 8 August, 2011

ACCEPTED 8 November, 2011

To test the salt specimens under elevated temperatures the prepared specimens and loading platens had been heated in an oven for 24 hours before testing. The low temperature specimens are achieved by cooling them in a freezer for 24 hours. The mechanical testing is performed immediately after removing them from the oven or freezer. The specimen installation, equipment setup and loading are completed within 4 minutes. The changes of specimen temperatures between before and after testing are less than 5 Kelvin. As a result the specimen temperatures are assumed to be uniform and constant with time during the mechanical testing (i.e., isothermal condition).

3. Strength Testing

A polyaxial load frame [10] has been developed to apply axial stress and lateral stresses to the cubical salt specimens (Figure 1). The test frame utilizes two pairs of cantilever beams to apply lateral stresses to the specimen. The axial stress is applied by a hydraulic cylinder connected to an electric pump. The frame has an advantage over the conventional triaxial (Hoek) cell because it allows a relatively quick installation of the test specimen under triaxial condition, and hence the change of the specimen temperature during testing is minimal. A total of ten specimens have been tested for each temperature level with the confining (lateral) stresses varying from 0, 3, 5, 10, 15, 20 to 30 MPa. They are loaded axially at a constant rate of 1 MPa/s until failure occurs.

Figure 2 shows stress-strain curves monitored from some of the salt specimens under various temperatures and confining pressures. For all specimens the two measured lateral strains induced by the same magnitude of the applied lateral stresses are similar. Some discrepancies may be due to the intrinsic variability of the salt.

The results indicate that the uniaxial compressive strengths (σ_c) of salt decrease linearly with increasing temperature (T) and can be represented best by (Figure 3 and Table 1):

$$\sigma_c = -0.067T + 56.7 \quad (1)$$

Table 2 shows the triaxial compressive strength results. Under the same confining pressure (σ_3) the maximum principal stress at failure (σ_1) decreases with increasing specimen temperature.

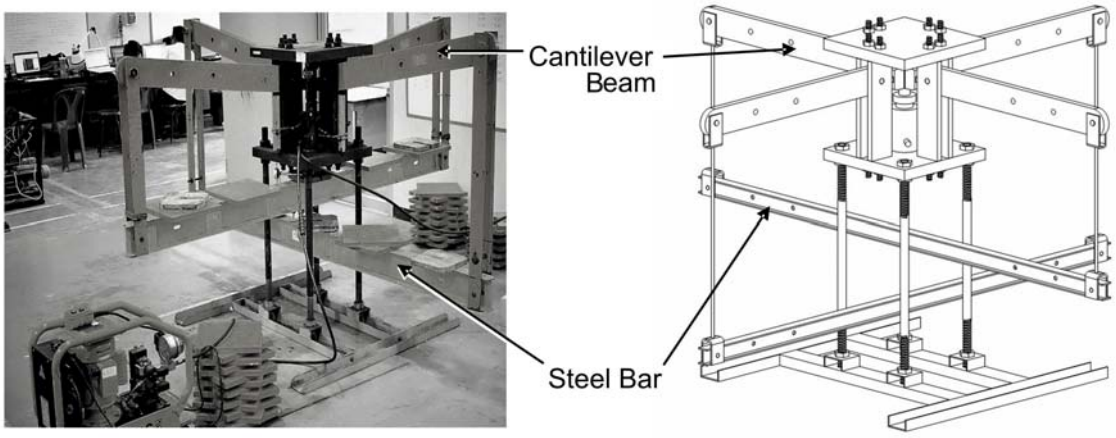

Figure 1 Polyaxial load frame used in the compressive strength testing of salt specimens under various temperatures.

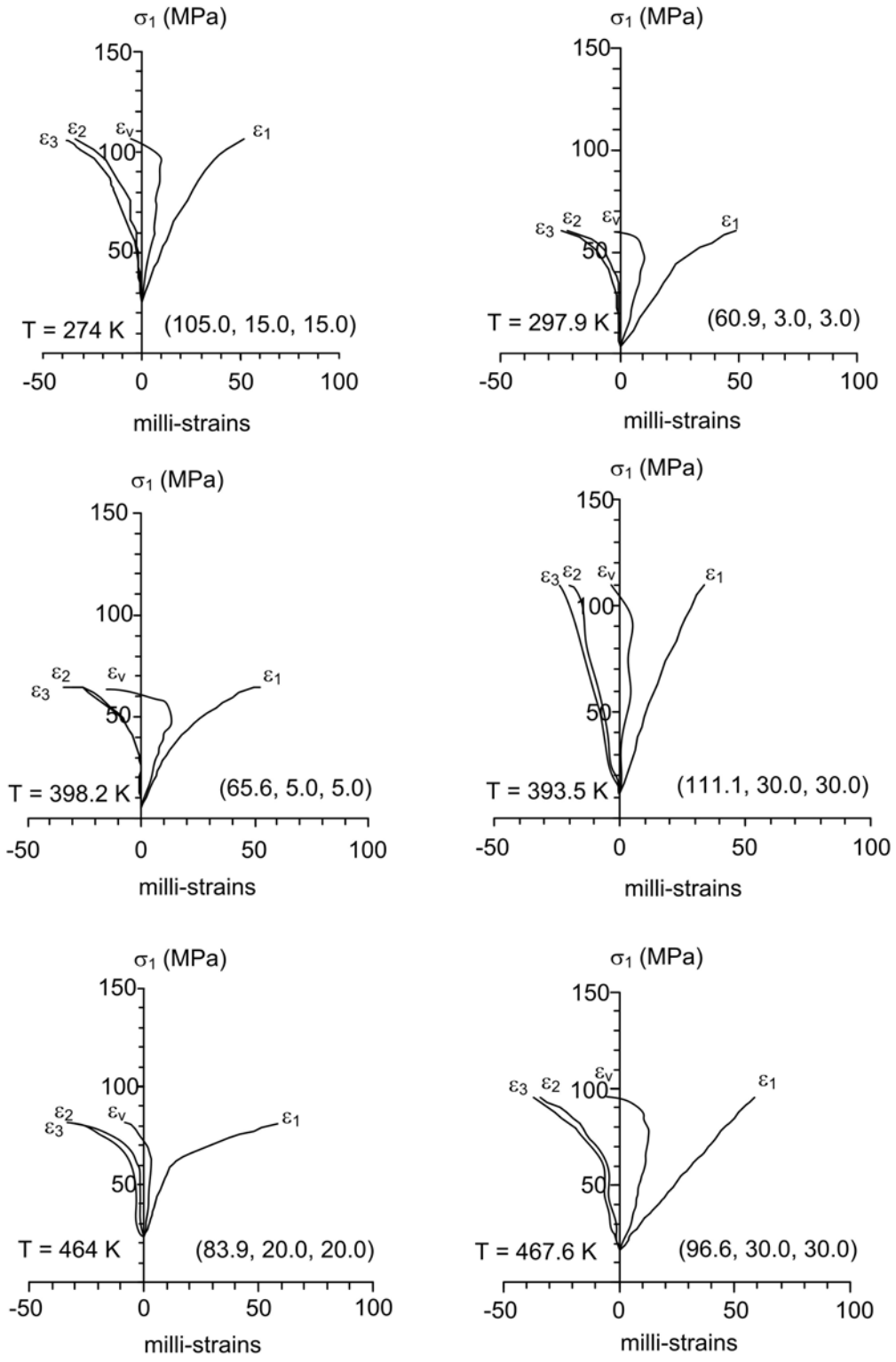

Figure 2 Stress-strain curves obtained from some salt specimens with different temperatures. Numbers in brackets indicate σ_1, σ_2 and σ_3 at failure.

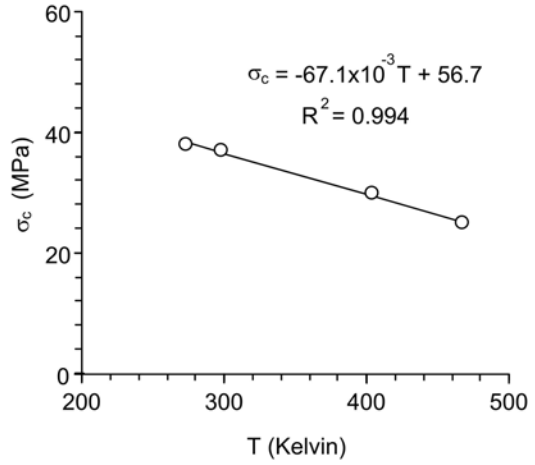

Figure 3 Uniaxial compressive strength of salt as a function of temperature

Table 1 Uniaxial compressive strengths of salt.

Specimen no.	Density, ρ (g/cc)	Temperature, T (Kelvin)	σ_c (MPa)
UCS 45-47	2.12 ± 0.03	277.0 ± 2.3	37.9 ± 3.0
UCS 81,87,90	2.00 ± 0.05	298.0 ± 0.6	37.0 ± 2.5
UCS 51-53	2.10 ± 0.01	394.0 ± 4.7	30.0 ± 3.5
USC 74	2.15	455.5	25

Table 2 Triaxial compressive strengths of salt.

σ_3 (MPa)	σ_1 (MPa)			
	Testing Temperature			
	274 K	280 K	404 K	467 K
1.6	49.0	45.9	-	-
3	63.6	60.9	52.5	-
5	77.9	76.8	65.6	50.0
10	96.6	93.0	80.6	67.4
15	109.5	105.0	88.9	77.1
20	118.6	113.3	96.0	83.9
30	135.0	128.5	111.0	97.1

The Brazilian tensile strength of the salt has been determined from disk specimens with temperatures ranging from 273, 298, 404 to 467 Kelvin. Except the pre-heating and cooling process, the test procedure, sample preparation and strength calculation follow the ASTM standard practice [11]. Table 3 shows the test results. The tensile strength (σ_B) decreases linearly with increasing specimen temperature (T), and can be represented by (Figure 4):

$$\sigma_B = -0.012T + 10.5 \quad (2)$$

The maximum principal stresses at failure (σ_1) from the compressive and tensile testing can be presented as a function of the minimum principal stress (σ_3) in Figure 5. Non-linear relations can be observed at all temperature levels. The higher temperature imposed on the salt specimen, the lower failure envelope is obtained.

Based on the Coulomb criterion the cohesion (c) and internal friction angle (ϕ) can be determined from the strength results for each temperature level using the following relations [12]:

$$\sigma_1 = \sigma_c + \sigma_3 \tan^2[(\pi/4)+(\phi/2)] \quad (3)$$

$$\sigma_c = 2 \cdot c \cdot \tan[(\pi/4)+(\phi/2)] \quad (4)$$

They are determined from the tangent of the σ_1 - σ_3 curves at σ_3 = 10 MPa. It is found that the cohesion and friction angle decrease linearly with increasing temperature (Figure 6) which agrees reasonably well with the linear drop of the uniaxial and tensile strengths as the temperature increases.

To incorporate the intermediate principal stress (σ_2) the test results can be presented in terms of the octahedral shear stress at failure (τ_{oct}) as a function of mean stress (σ_m), as shown in Figure 7, where [12]:

$$\tau_{oct} = \left\{\frac{1}{3}\left[(\sigma_1-\sigma_2)^2+(\sigma_2-\sigma_3)^2+(\sigma_3-\sigma_1)^2\right]\right\}^{1/2} \quad (5)$$

$$\sigma_m = \frac{1}{3}(\sigma_1+\sigma_2+\sigma_3) \quad (6)$$

The diagram in Figure 7 clearly indicates that the effect of temperature on the salt strength is larger when the salt is under higher confining pressures. When σ_m is below 20 MPa, the octahedral shear stresses required to fail the salt specimen are less sensitive to the temperature variation.

Table 3 Brazilian Tensile Strengths of Salt.

Specimen No.	Density, ρ (g/cc)	Temperature, T (Kelvin)	σ_B (MPa)
BZ 1-10	2.12 ± 0.01	274.0 ± 3.1	7.3 ± 0.51
BZ 11-20	2.10 ± 0.05	297.5 ± 0.8	6.0 ± 0.60
BZ 21-30	2.21 ± 0.04	393.7 ± 5.1	5.8 ± 0.84
BZ 31-40	2.09 ± 0.04	464.7 ± 4.5	4.8 ± 0.42

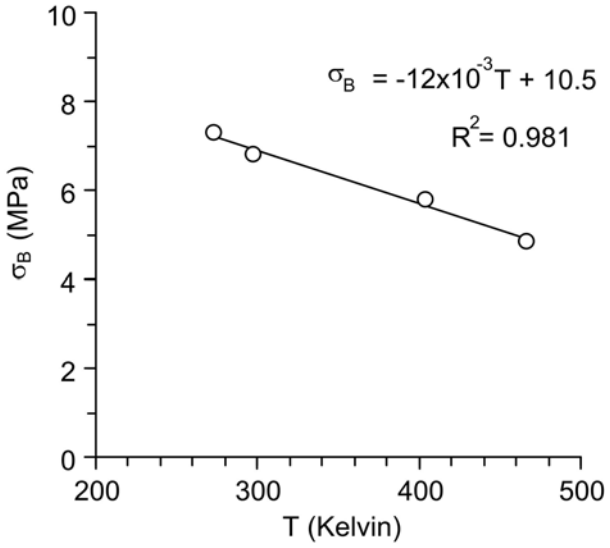

Figure 4 Brazilian tensile strength of salt as a function of temperature

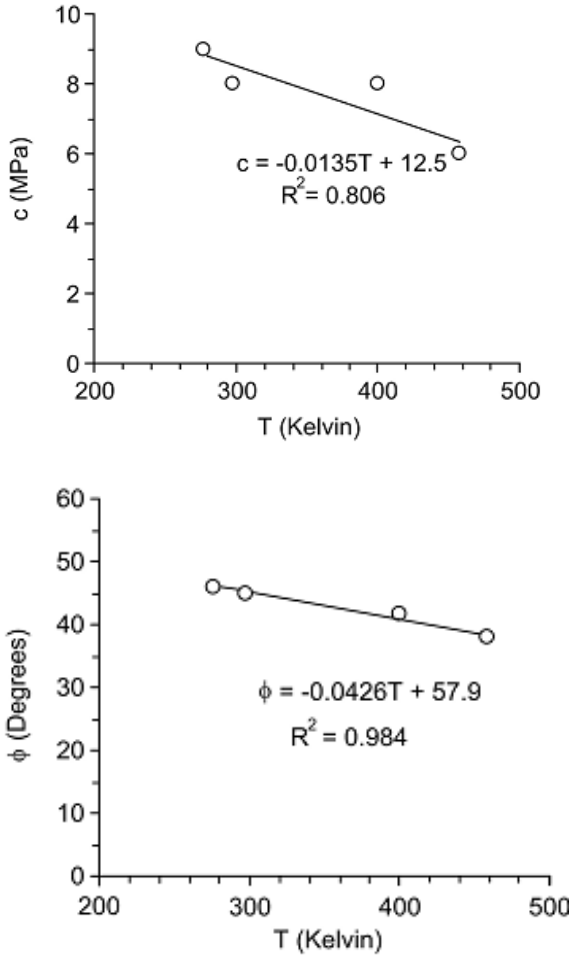

Figure 6 Cohesion and internal friction angle of salt as a function of temperature.

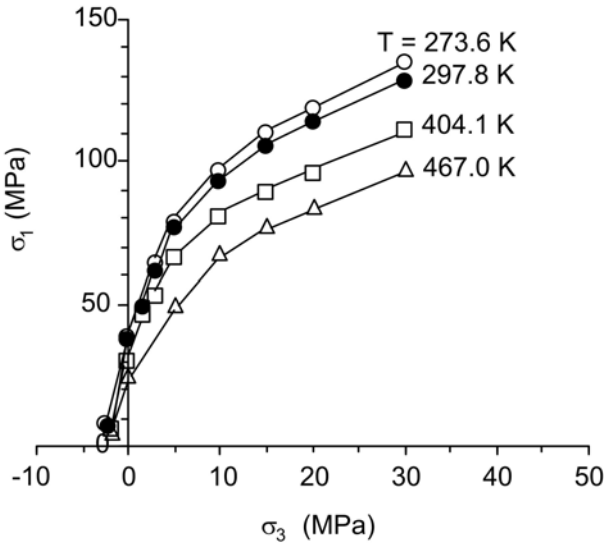

Figure 5 Major principal stress at failure as a function of confining pressure.

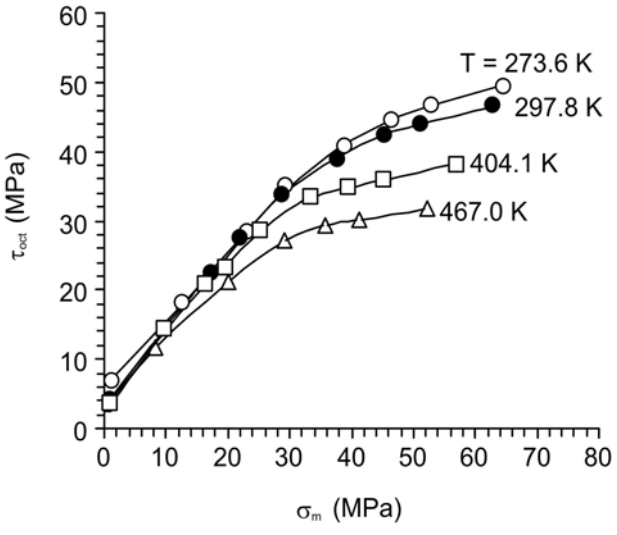

Figure 7 Octahedral shear strength of salt as a function of mean stress.

4. Strain Energy Density Criterion

The strain energy density principle is applied here to describe the salt strength and deformability under different temperatures. It is assumed that under a given mean strain energy and temperature the distortional strain energy required to fail the salt specimens are constant. Regression on the test results shows that the distortional strain energy (W_d) increases linearly with the mean strain energy (W_m):

$$W_d = A \cdot W_m + B \tag{7}$$

The parameters A and B are empirical constants depending on the strength and cohesion of the salt under each temperature. They can be determined by regression analysis on the test data, as shown in Figure 8. It is interesting to note that the increasing rates of W_d with respect to W_m are virtually the same for all temperature levels. At a given mean strain energy the higher temperature results in a lower distortional strain energy required to fail the salt specimen.

Assuming that for each temperature level the salt is linearly elastic prior to failure, W_d and W_m can be determined for each specimen using the following relations (Table 4) [12]:

$$W_d = \frac{3}{4}\left(\frac{\tau_{oct}^2}{G}\right) \tag{8}$$

$$W_m = \left(\frac{\sigma_m^2}{2K}\right) \tag{9}$$

The elastic parameters G and K can be defined as a function of the testing temperature, and hence the salt strengths from different temperatures can be correlated. Table 4 summarizes the measurement results for each specimen in terms of the elastic modulus (E), shear modulus (G), bulk modulus (K) and Poisson's ratio (ν). Linear variations of the four parameters with respect to temperature are observed from the results, as shown in Figure 9. Good correlations are obtained when they are fitted with the following linear equations:

$$E = -0.06T + 42.7 \tag{10}$$

$$G = -0.0215T + 16.2 \tag{11}$$

$$K = -0.0254T + 35.6 \tag{12}$$

$$\nu = (7\times10^{-6})T + 0.33 \tag{13}$$

The results suggest that the elastic, shear and bulk moduli decrease with increasing temperature. The Poisson's ratio however tends to be independent of the temperature. By substituting equations (11) into (8) and (12) into (9) the W_d at failure can therefore incorporate the effect of specimen temperature into the strength calculation.

The distortional strain energy for each salt specimen at failure, that implicitly takes the temperature effect into consideration, is plotted as a function of the mean strain energy in Figure 10. The data can be described best by a linear equation:

$$W_d = A_{Th} \cdot W_m + B_{Th} \tag{14}$$

The parameters A_{Th} and B_{Th} are empirical constants depending on the strength and thermal response of the rock. For the Maha Sarakham salt A_{Th} = 1.53 and B_{Th} = 63.7 MPa. A good correlation is obtained between the test results and the proposed criterion (R^2 = 0.851).

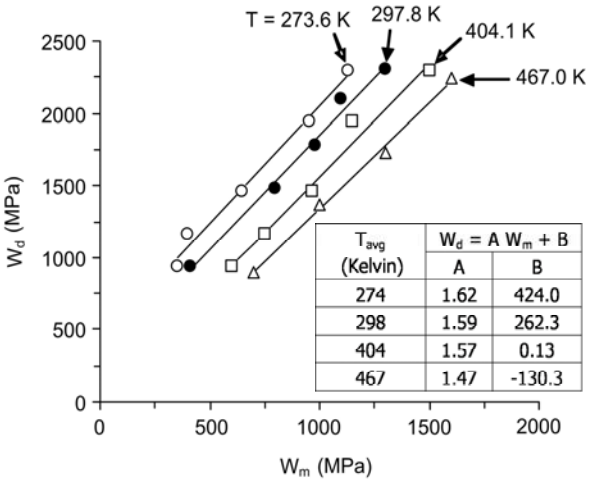

Figure 8 Distortional strain energy at failure as a function of mean strain energy.

Table 4 Elastic parameters and strain energy density at failure.

T_{avg} (Kelvin)	σ_m (MPa)	τ (MPa)	E (GPa)	ν	G (GPa)	K (GPa)	W_d (MPa)	W_m (MPa)
274	23.2	28.6	27.1	0.38	9.8	37.6	-	-
	29.3	34.4	29.1	0.42	10.2	60.6	-	-
	38.9	40.8	28.7	0.32	10.9	26.6	893.6	700.0
	46.5	44.5	29.1	0.34	10.9	30.3	1368.6	1000.0
	52.9	46.5	27.1	0.37	9.9	34.7	1725.2	1300.0
	65.0	49.5	29.5	0.35	10.9	32.8	2242.2	1600.0
	Mean ± SD		28.4 ± 0.9	0.36 ± 0.04	10.4 ± 0.4	37.1 ± 3.2		
298	17.4	22.3	21.0	-	-	-	-	-
	22.3	27.3	27.0	0.35	10.0	30.0	-	-
	28.9	33.8	26.8	0.36	9.9	31.9	935.6	600.0
	37.7	39.1	27.5	0.31	10.5	24.1	1158.5	750.0
	45.0	42.4	24.0	0.34	9.0	24.2	1458.0	970.0
	51.1	44.0	21.5	0.34	8.0	22.4	1944.0	1150.0
	62.8	46.4	26.4	0.37	9.6	33.8	2292.0	1500.0
	Mean ± SD		25.5 ± 2.1	0.34 ± 0.02	9.5 ± 0.8	27.8 ± 4.8	-	-
404	16.4	20.9	18.7	-	-	-	-	-
	19.5	23.3	20.1	0.36	7.4	23.9	-	-
	25.2	28.6	22.3	0.42	8.1	31.0	940.4	413.5
	33.5	33.3	19.8	0.41	7.0	36.7	1479.6	800.0
	39.6	34.8	17.5	0.30	6.6	17.2	1779.4	979.3
	45.3	35.8	20.9	0.32	7.9	19.4	2100.0	1100.0
	57.0	38.2	21.1	0.35	7.8	23.4	2300.0	1300.0
	Mean ± SD		20.0 ± 1.5	0.37 ± 0.05	7.5 ± 0.5	25.3 ± 7.3	-	-
467	20.0	21.2	17.5	0.36	6.4	20.8	935.6	350.0
	29.1	27.1	16.2	0.34	6.0	16.9	1158.5	400.0
	35.7	29.3	18.5	0.40	6.6	30.8	1458.0	650.0
	41.3	30.1	20.0	0.36	7.4	23.8	1944.0	955.0
	52.4	31.6	17.3	0.34	6.5	18.0	2292.0	1132.0
	Mean ± SD		18.1 ± 1.4	0.36 ± 0.02	6.6 ± 0.47	22.1 ± 5.58	-	-

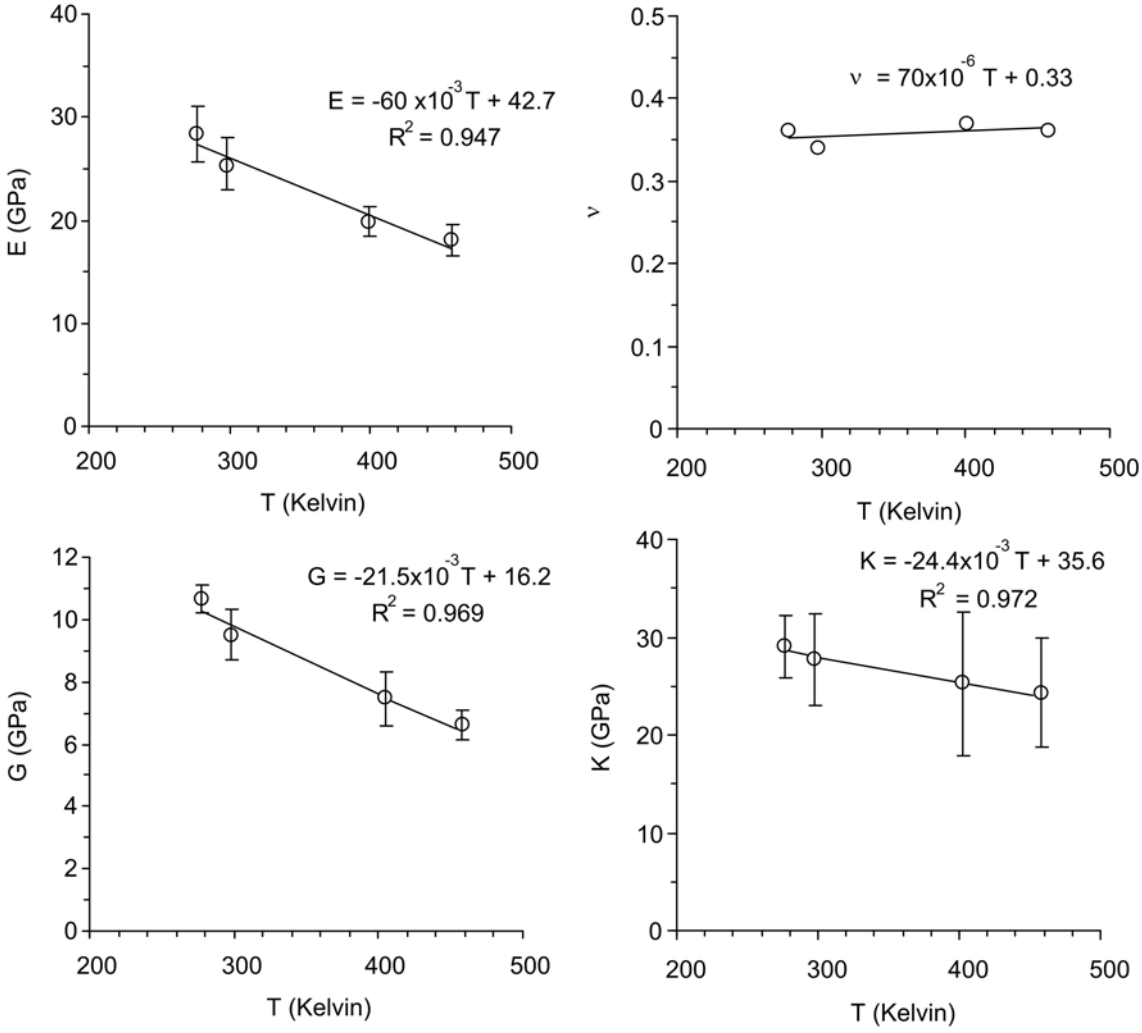

Figure 9 Elastic parameters of salt as a function of temperature.

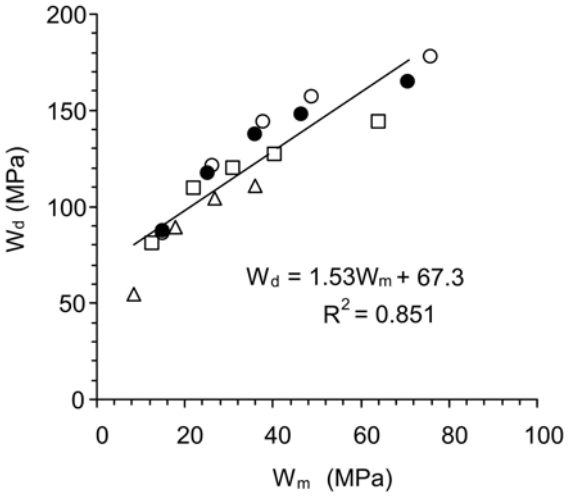

Figure 10 Distortional strain energy with temperature consideration as a function of mean strain energy.

5. Discussions and Conclusions

This study experimentally determines the salt strengths under different constant temperatures separately. For each temperature level the testing is assumed to be under isothermal condition (constant temperature with time during loading). For this simplified approach the salt specimens subject to different temperatures have been taken as different materials. As a result the induced thermal stress or thermal energy imposed on the salt specimens has not been explicitly incorporated into the initial strength calculation. This approach is different from the conventional thermo-mechanical analysis.

The decrease of the salt strength as the temperature increases suggest that the applied thermal energy before the mechanical testing makes the salt weaker, and more plastic – failing at lower stress and higher strain with lower elastic and shear moduli. The temperature effect is larger when salt is under higher mean stress. In order to consider the temperature dependency of the failure stress and strain and elastic properties the strain energy density concept is applied. Assuming that the salt is linearly elastic before failure, the distortional strain energy (W_d) at failure can be calculated as a function of mean strain energy, W_m (Figure 8). In Figure 8 at a given W_m the W_d decreases with increasing temperature. The differences of W_d from one temperature to the other therefore correspond to the difference of thermal energy imposed on the specimens.

The single multi-axial strength criterion [14] for salt under various confining pressures and temperatures implicitly considers the effect of the thermal energy by incorporating the empirical equations between the elastic parameters and temperature into the $W_d - W_m$ relation (Figure 9). The strain energy criterion agrees well with the strength results from different temperature levels (Figure 10). Since the analysis is intended to determine the short-term strength, the creep deformations induced by the mechanical and thermal loadings are not considered here.

The proposed criterion can be used to determine the stability of rock salt around compressed-air or gas storage caverns during product injection (high temperature, low deviatoric stress) and withdrawal (low temperature, high deviatoric stress). The effect of temperature on the salt strength may be enhanced for the salt cavern with high frequency of injection-retrieval cycles. To be conservative the maximum temperature (induced during injection) and the maximum shear stresses (induced during withdrawal) in salt around the cavern should be determined (normally by numerical simulation). The salt stability can be determined by comparing the computed temperature distribution and mechanical and thermal stresses against the criterion proposed above. The results should lead to a conservative design of the safe maximum and minimum storage pressures.

This study is funded by Suranaree University of Technology. Permission to publish this paper is gratefully acknowledged. We would like to thank Pimai Salt Co. who donates salt cores for testing.

6. Acknowledgements

The work was funded by Suranaree University of Technology. Permission to publish this paper is gratefully acknowledged. We would like to thank Pimai Salt Co. for donating salt cores used in this study.

References

[1] H. Vosteen and R. Schellschmidt, “Influence of temperature on thermal conductivity, thermal capacity and thermal diffusivity for different types of rock,” Physics and Chemistry of the Earth, Parts A/B/C, 28, No. 9-11 (2003).

[2] M. Shimada and J. Liu, “Temperature dependence of strength of rock under high confining pressure,” Annuals of Disas., Prev. Res. Inst., No. 43B-1 (2000).

[3] R. P. Okatov, F. K. Nizametdinov, B. N. Tsai, and T. T. Bondarenko, “Time and temperature factors in construction of rock strength criteria,” Journal of Mining Science, 39, No. 2 (2003).

[4] N. L. Carter and F. D. Hansen “Creep of rocksalt at elevated temperature,” in: Proceedings of the 21st US Symposium on Rock Mechanics, Rolla, Missouri (1980).

[5] W. G. Liang, S. G. Xu, and Y. S. Zhao, “Experimental study of temperature effects on physical and mechanical characteristics of salt rock,” Rock Mechanics and Rock Engineering, 39, No. 5 (2006).

[6] H. W. Duddeck and H. K. Nipp, “Time and temperature dependent stress and displacement fields for salt domes,” in: Proceedings of the 23rd Symposium on Rock Mechanics, Berkeley, Publ New York: AIME (1982).

[7] J. Warren, Evaporites: Their evolution and economics, Blackwell Science, Oxford (1999).

[8] K. Fuenkajorn and S. Archeeploha, “Prediction of salt cavern configurations from subsidence data,” Engineering Geology, 110, No. 1-2 (2009).

[9] K. Fuenkajorn and D. Phueakphum, “Effects of cyclic loading on mechanical properties of Maha Sarakham salt,” Engineering Geology, 112, No. 1-4 (2010).

[10] T. Sriapai, P. Samsri, and K. Fuenkajorn, “Polyaxial strength of Maha Sarakham salt,” in: Proceedings of The third Thailand Symposium on Rock Mechanics, Suranaree University of Technology, Nakhon Ratchasima (2011).

[11] ASTM D3967-08, “Standard test method for splitting tensile strength of intact rock core specimens,” Annual Book of ASTM Standards, 04.08, ASTM International, West Conshohocken, PA (2008).

[12] J. C Jaeger, N. G. W. Cook and, R. W. Zimmerman, Fundamentals of Rock Mechanics, Fourth Edition, Blackwell Publishing, Oxford (2007).